Effect of cholesterol on the transfection efficiency of DOTAP-containing lipoplexes

Daniela Pozzi,[*] Francesco Cardarelli,[**] Fabrizio Salomone,[**] Cristina Marchini,[***] Heinz Amenitsch,[****] and Giulio Caracciolo[*]

[*]Department of Molecular Medicine, "Sapienza" University of Rome, Viale Regina Elena 324, 00161, Rome, Italy
[**]Center for Nanotechnology Innovation @NEST, Istituto Italiano di Tecnologia, Piazza San Silvestro 12, 56127 Pisa, Italy
[***]Department of Bioscience and Biotechnology, University of Camerino, Via Gentile III da Varano, 62032 Camerino (MC), Italy
[****]Institute of Inorganic Chemistry, Stremayrgasse 9, 8010 GrazGraz University of Technology, Graz, Austria

ABSTRACT

Most lipid formulations need cholesterol for efficient transfection, but the precise motivation remains unclear. Here, we have investigated the effect of cholesterol on the transfection efficiency (TE) of cationic liposomes made of 1,2-dioleoyl-3-trimethylammonium-propane (DOTAP) and dioleoylphosphocholine (DOPC) in Chinese hamster ovary cells. The transfection mechanisms of cholesterol-containing lipoplexes have been investigated by TE, synchrotron small angle X-ray scattering (SAXS) and laser scanning confocal microscopy (LSCM) experiments. We prove that cholesterol-containing lipoplexes enter the cells using different endocytosis pathways. Formulations with high cholesterol content efficienlty escape from endosomes. These studies will contribute to the rational design of novel lipid nanocarriers with superior TE.

Keywords: cationic liposome, lipoplexes, cholesterol, transfection efficiency, confocal microscopy

1 INTRODUCTION

Nowadays, cationic liposomes (CLs) are among the most promising candidates for in vivo and ex vivo delivery of nucleic acids [1, 2]. The low transfection efficiency (TE) of CL-DNA complexes (lipoplexes) is due to the multiple intracellular barriers that they must overcome to deliver exogenous DNA into the cell nucleus of the host cell and enable its expression [3]. Depending on the mode of cellular uptake, lipoplexes can be shuttled to lysosomes, recycled back to the plasma membrane, or delivered to other subcellular compartments. Recently, it has been suggested that internalization pathways of lipoplexes are cholesterol-dependent and that cholesterol plays a major role on their intracellular trafficking [4]. The incorporation of cholesterol and cholesterol-derivatives in the lipoplex formulation has been shown to boost TE [5-7], but the precise mechanism through which this occurs still deserves further investigation. To this end, here we address the transfection mechanisms of cholesterol-containing lipoplexes. We used CLs made of the cationic 1,2-dioleoyl-3-trimethylammonium-propane (DOTAP) and the neutral dioleoylphosphocholine (DOPC), and we gradually replaced DOPC molecules by cholesterol. Employing structural studies by synchrotron small angle X-ray scattering (SAXS), laser scanning confocal microscopy (LSCM) and TE measurements, we were able to elucidate the relation between efficiency and transfection mechanism of cholesterol-containing lipoplexes.

2 MATERIALS AND METHODS

2.1 Liposomes preparation

1,2-dioleoyl-3-trimethylammonium-propane (DOTAP) and dioleoylphosphocholine (DOPC) were purchased from Avanti Polar Lipids (Alabaster, AL, USA) and used without further purification. Cholesterol was purchased in powder form from Sigma-Aldrich (St. Louis, MO, USA). All mixtures were prepared at molar fractions of cationic lipid in the bilayer X_{DOTAP}=0.5 and at molar fractions of neutral lipid in the bilayer $X_{DOPC}+X_{Chol}$=0.5, but gradually replacing DOPC molecules with cholesterol molecules. Five different mixtures were prepared with increasing molar fractions of cholesterol (X_{Chol}=0, 0.125, 0.25, 0.375, 0.5). Each mixture was dissolved in chloroform and the solvent was evaporated under vacuum for at least 24 h. The obtained lipid films were hydrated with the appropriate amount of Tris–HCl buffer solution (10^{-2} M, pH 7.4) to achieve the desired final concentration (1 mg ml^{-1} for all the experiments except for SAXS experiments where it was 10 mg ml^{-1}).

2.2 Lipoplexes preparation

For transfection experiments, plasmid DNA (pGL3 which codifies for firefly luciferase; Promega, Madison, WI,

USA) was employed. For SAXS experiments, calf thymus DNA (Sigma-Aldrich, St. Louis, MO, USA) was used. For confocal fluorescence microscopy experiments, Cy5-labeled 2.7-kbp plasmid DNA (Mirus Bio Corporation, Madison, WI, USA) was used. By mixing adequate amounts of the DNA solutions to suitable volumes of liposome dispersions, self-assembled lipoplexes were obtained. All the experiments were performed at charge ratio ρ=cationic lipid/DNA (mol/mol)=3.

2.3 Transfection efficiency experiments

Cell lines were cultured in Dulbecco's modified Eagle's medium (DMEM) with Glutamax-1 (Invitrogen, Carlsbad, CA, USA) supplemented with 1% penicillin–streptomycin (Invitrogen) and 10% fetal bovine serum (Invitrogen) at 37 °C and 5% CO_2 atmosphere, splitting the cells every 2–4 days to maintain monolayer coverage. For luminescence analysis, Chinese hamster ovary (CHO) cells were transfected with pGL3 control plasmid (Promega, Fitchburg, WI, USA). The day before transfection, cells were seeded in 24-well plates (150,000 cells per well) using medium without antibiotics. Cells were incubated until they were 75–80% confluent, which generally took 18–24h. For TE experiments, lipoplexes were prepared in Optimem (Invitrogen) by mixing for each well of 24-well plates 0.5 μg of plasmid with 5 μl of sonicated lipid dispersions (1 mg ml^{-1}). Complexes were left for 20 min at room temperature before adding them to the cells. On the day of transfection, the growth medium was replaced with 400 μl of Optimem and the cells were incubated for 30 min at 37 °C before adding 100 μl of lipoplexes in Optimem. Cells were incubated at either 37 °C for an additional 4 h to permit transient transfection. Finally, to avoid internalization of complexes that could remain bound to the cell surface after medium replacement, the cells were extensively washed 3× with phosphate buffered saline (PBS) at 37 °C before DMEM medium supplemented with 10% fetal bovine serum at 37 °C was added. After 48 h, cells were analyzed for luciferase expression using Luciferase Assay System from Promega. Briefly, cells were washed in PBS and harvested in 200 μl 1× reporter lysis buffer (Promega). Of the cell suspension, 20 μl was diluted in 100 μl luciferase reaction buffer (Promega) and the luminescence was measured 10 s using a Berthold AutoLumat luminometer LB-953 (Berthold, Bad Wildbad, Germany). Results were expressed as relative light units per mg of cell proteins as determined by Bio-Rad Protein Assay Dye Reagent (Bio-Rad, Hercules, CA, USA). Each condition was performed in quadruple and repeated three times.

2.4 Synchrotron small angle X-ray scattering

SAXS measurements were performed at the Austrian SAXS station of the synchrotron light source ELETTRA (Trieste, Italy). SAXS patterns were recorded with gas detectors based on the delay line principle covering the q-ranges from q_{min} = 0.04 $Å^{-1}$ to q_{max} = 0.5 $Å^{-1}$ with a resolution of 5 × 10^{-4} $Å^{-1}$ (fwhm). The angular calibration of the detectors was performed with silver behenate powder (d-spacing of 58.38 Å). The data have been normalized for variations of the primary beam intensity, corrected for the detector efficiency, and the background has been subtracted. Exposure times were typically 300 s. No evidence of radiation damage was observed in the X-ray diffraction patterns. The sample was held in a 1 mm glass capillary (Hilgenberg, Malsfeld, Germany) and the measurements were performed at 25 °C with a precision of 0.1 °C.

2.5 Cell culture, transfection, and colocalization assays

CHO-K1 were purchased from American Type Culture Collection (CCL-61 ATCC) and were grown in Ham's F12K medium supplemented with 10% of fetal Bovine Serum at 37 °C and in 5% CO2. For transfection experiments, lipoplexes were prepared in PBS (Invitrogen) by mixing 1 μl of Cy3-labeled DNA with 10 μl of sonicated lipid dispersions. These complexes were left for 20 min at room temperature before adding them to the cells. In order to identify the endocytic vesicles involved in lipoplex internalization, we performed colocalization assays in living cells. CHO-K1 cells were coincubated with lipoplexes and different endocytic fluorescent markers: 1 mg/ml 70 kDa dextran-fluorescein isothiocyanate (FITC) conjugate at 37 °C for 30 min to label macropinosomes, 50 mM Lysosensor for 30 min to label lysosomes, 2 μg/ml transferrin-Alexa488 conjugate for 30 min to label recycling and sorting endosomes. Transfection of Caveolin-GFP was carried out using lipofectamine reagent (Invitrogen) according to the manufacturer's instruction. Colocalization of green and red signals was analyzed using the "colocalization finder" plugin of the ImageJ software (NIH Image; http://rsbweb.nih.gov/ij/) [8].

2.6 LSCM experiments

Laser scanning confocal microscopy (LSCM) experiments were performed with the Olympus Fluoview 1000 (Olympus, Melville, NY) confocal microscope interfaced with a 405 nm diode laser, a 488 nm Argon laser, and 543 nm helium-neon laser. Glass bottom Petri dishes containing transfected cells were mounted in a temperature-controlled chamber at 37 °C and 5% CO_2 and viewed with a 60×1.25 numerical aperture water immersion objective. The following collection ranges were adopted: 500–540nm (EGFP, Alexa488-transferrin and FITC-Dextran70 kDa), 555–655 nm (Cy3) and 460–530 (Lysosensor). Images were collected in sequential mode to eliminate emission cross talk between the various dyes.

3 RESULTS AND DISCUSSION

3.1 Transfection efficency

Fig.1 shows the TE of DOTAP–DOPC–cholesterol/DNA lipoplexes (ρ=3) at five molar fractions of neutral cholesterol in the lipid bilayer (X_{Chol}=0, 0.125, 0.25, 0.375, 0.5). The charge was kept constant by fixing the molar fraction of cationic lipid (X_{DOTAP}=0.5), while neutral DOPC molecules were gradually replaced by cholesterol. Fig.1 shows that incorporation of cholesterol results in a marked enhancement of TE. To rationalize the TE behvaiour of cholesterol-containing lipoplexes, we first characterized the phase organization of DOTAP–DOPC–cholesterol/DNA lipoplexes at the nanoscale. Indeed, it is known that the nanostructure of lipoplexes might correlate with their TE.

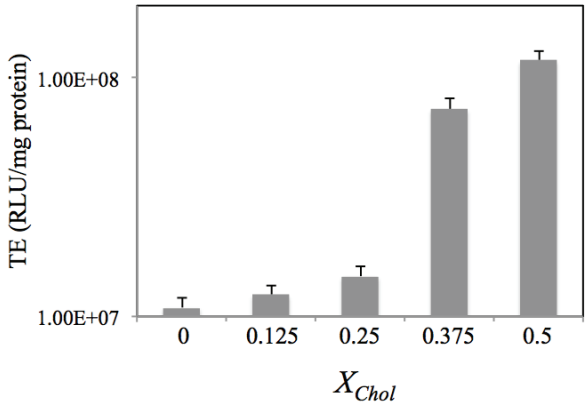

Figure1: Transfection efficiency (TE) in RLU per mg of cellular proteins of DOTAP–DOPC-cholesterol/DNA lipoplexes as a function of increasing molar fractions of cholesterol, X_{Chol}.

3.2 Nanostructure

Fig. 2 (panel A) shows two representative synchrotron SAXS patterns of DOTAP–DOPC–cholesterol/DNA (X_{Chol}=0 and 0.5) at ρ=3. The sharp peaks at q_{00l} are due to alternating lipid bilayer–DNA–monolayer multilamellar structure with periodicity $d=2\pi/q_{00l}$. The broad peak marked by an arrow results from one-dimensional (1D) ordering of the DNA sandwiched between the lipid bilayers. It is usually referred to as "DNA peak" and corresponds to a DNA interhelical spacing $d_{DNA} = 2\pi/q_{DNA}$. Fig. 2 (panels B and C) shows the variation of d and d_{DNA} as a function of the molar fraction of cholesterol, X_{Chol}. We observed that the interlamellar periodicity d decreased less then 1 Å with increasing X_{Chol} (Fig. 2, panel B), due to the reduced hydration layer of cholesterol molecules. Reduction in the DNA interhelical spacing are due to the reduction in membrane area where DNA condensation occurs (headgroup area of cholesterol is definitely smaller than that of DOPC). However, no evidence of phase transition was found. Thus, we asked whether differences in TE could be due differences in the uptake mechanism and/or in the final fate of lipoplexes.

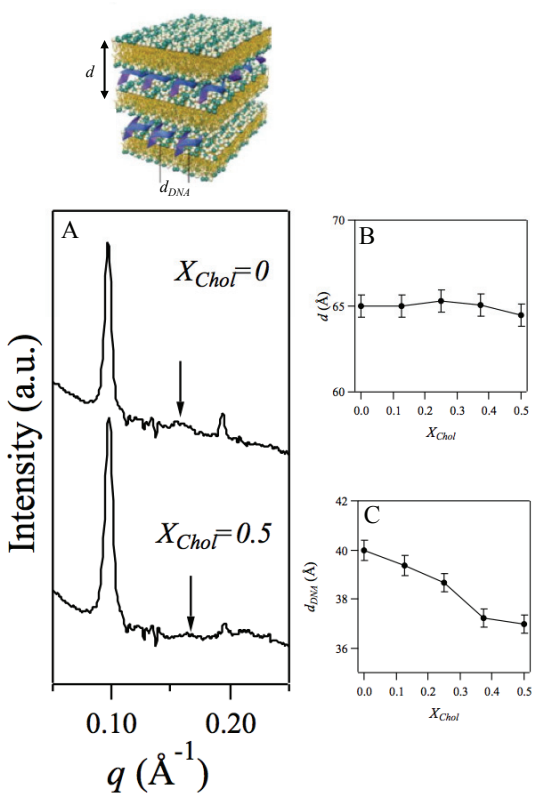

Figure 2: (A) Representative synchrotron SAXS patterns of lipoplexes. Lamellar periodicity (B) and DNA-DNA distance (C) of cholesterol-containing lipoplexes. At the top of panel A a schematic of the multilamellar structure of lipoplexes is shown.

3.2 Uptake mechanism

To investigate the uptake mechanisms of lipoplexes in CHO cells, LSCM experiments were performed on DOTAP–DOPC/DNA and DOTAP–cholesterol/DNA lipoplexes, as these formulations show the largest difference in the cholesterol content (X_{Chol}=0 and 0.5, respectively). Colocalization analysis of fluorescence signals from labeled lipoplexes (red) and various endocytic markers (green) was performed (Fig. 3). Remarkably, LSCM shows that, while DOTAP-DOPC/DNA lipoplexes enter CHO cells exclusively through fluid-phase macropinocytosis, cholesterol-containing lipoplexes can use different endocytosis pathways (caption to Fig. 3).

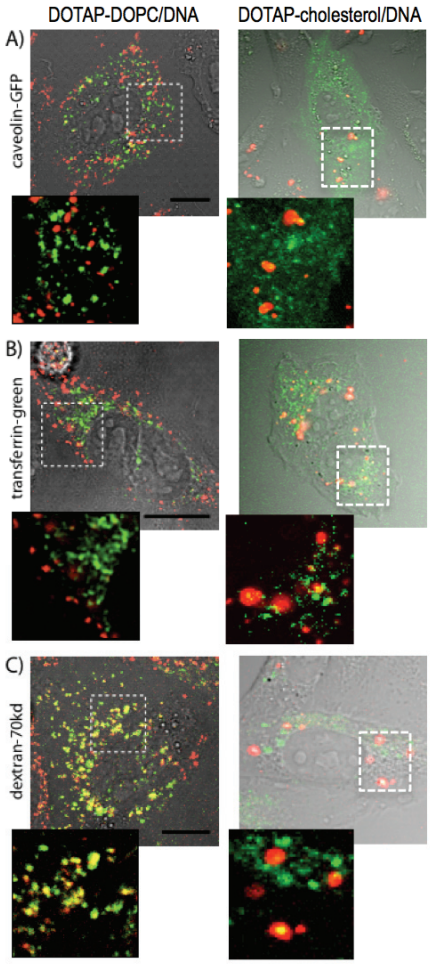

Figure 3: Colocalization of DOTAP-DOPC/DNA and DOTAP-cholesterol/DNA signals (red) with endocytic markers (green). For DOTAP-DOPC/DNA lipoplexes no colocalization was observed with caveolin- E1GFP (caveolar pathway) (A) and Alexa488-transferrin (clathrin pathway) (B) while high correlation (yellow vesicles) was observed with 70kDa dextran (macropinocytosis). On the opposite, DOTAP-cholesterol/DNA lipoplexes use all the endocytosis pathways to enter CHO cells.

3.3 Intracellular final fate

To account for the observed differences in TE, the ultimate intracellular fate of lipoplexes was finally evaluated. To this end, colocalization of DOTAP-DOPC/DNA and DOTAP–cholesterol/DNA lipoplexes with Lysosensor (lysosome marker, green) was investigated (Fig. 4). While DOTAP-DOPC/DNA lipoplexes kept their vesicular staining and were exclusively found in the lysosomes, the observation of large (μm-sized) red patches suggests that cholesterol-enriched lipoplexes are more fusogenic and most likely capable of efficient and early escape from endosomes [9].

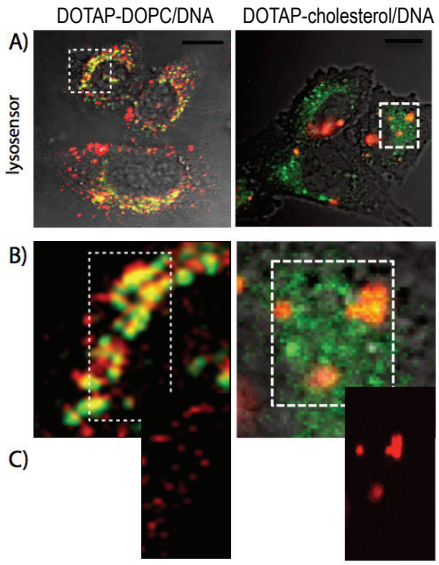

Figure 4: Colocalization of DOTAP-DOPC/DNA and DOTAP-cholesterol/DNA signals (red) with Lysosensor (lysosome marker, green), after 3 h of lipoplex treatment.

In conclusion, we have shown that cholesterol-containing lipoplexes can enter cells through different endocytosis pathways and largely avoid lysosomal degradation. Activation of multiple endocytic pathways and efficient endosomal escape may therefore explain the enhanced TE of cholesterol-based formulations. The mechanisms of action of cholesterol-containing nanocarriers should be considered for the rational design of novel systems with superior delivery efficiency.

REFERENCES

[1] C.R. Dass, J. Mol. Med., 82, 579–591, 2004.
[2] Guo, L. Huang, Acc. Chem. Res. DOI: http://dx.doi.org/10.1021/ar200151m.
[3] A. Elouahabi, J.M. Ruysschaer, Mol. Ther., 11, 336–347, 2005.
[4] J. Rejman, V. Oberle, I.S. Zuhorn, D. Hoekstra, Biochem. J., 377, 159–169, 2004.
[5] A.P. Dabkowska, D.J. Barlow, A.V. Hughes, R.A. Campbell, P.J. Quinn, M.J. Lawrence, J. R. Soc. Interface, 9 548–561, 2012.
[6] L. Xu, T.J. Anchordoquy, Mol. Pharm., 7, 1311–1317, 2010.
[7] F. Koster, D. Finas, C. Schulz, C. Hauser, K. Diedrich, R. Felberbaum, Int. J. Mol. Med., 14, 769–772, 2004.
[8] V. Zinchuk, O. Zinchuk, T. Okada, Acta Histochem. Cytochem., 40, 101–111, 2007.
[9] D. Pozzi, C. Marchini, F. Cardarelli, H. Amenitsch, C. Garulli, A. Bifone, G. Caracciolo, Biochim. Biophys. Acta, 1818, 2335-2343, 2012.